Thrombosis and Haemostasis

THE D173G MUTATION IN ADAMTS-13 CAUSES A SEVERE FORM OF CONGENITAL THROMBOTIC THROMBOCYTOPENIC PURPURA: A CLINICAL, BIOCHEMICAL AND IN SILICO STUDY

Journal:	*Thrombosis and Haemostasis*
Manuscript ID:	TH-15-02-0119.R2
Manuscript Type:	Original Article: Coagulation and Fibrinolysis
Category:	Basic Science
Date Submitted by the Author:	19-Jun-2015
Complete List of Authors:	Lancellotti, Stefano; Catholic University School of Medicine, Internal Medicine and Medical Specialties Peyvandi, Flora; Regina Elena Foundation and University of Milan, 2Angelo Bianchi Bonomi Hemophilia and Thrombosis Center and Fondazione Luigi Villa, IRCCS Maggiore Hospital, Mangiagalli Pagliari, Maria Teresa; Regina Elena Foundation and University of Milan, 2Angelo Bianchi Bonomi Hemophilia and Thrombosis Center and Fondazione Luigi Villa, IRCCS Maggiore Hospital, Mangiagalli Cairo, Andrea; Regina Elena Foundation and University of Milan, 2Angelo Bianchi Bonomi Hemophilia and Thrombosis Center and Fondazione Luigi Villa, IRCCS Maggiore Hospital, Mangiagalli Abdel-Azeim, Safwat; King Abdullah University of Science and Technology, Kaust Catalysis Center Edrisse Chermak, Edrisse; King Abdullah University of Science and Technology, Kaust Catalysis Center Lazzareschi, Ilaria; Catholic University of Sacred Heart, School of Medicinene, Rome, Italy, Pediatrics Mastrangelo, Stefano; Catholic University of Sacred Heart, School of Medicinene, Rome, Italy, Pediatrics Cavallo, Luigi; King Abdullah University of Science and Technology, Kaust Catalysis Center Oliva, Romina; University "Parthenope" of Naples, Sciences and Technologies De Cristofaro, Raimondo; Catholic University Sacred Heart School of Medicine, Medical Sciences
Keywords:	ADAMS/ADAMTS 13, Thrombotic thrombocytopenic purpura (TTP / HUS), Von Willebrand factor, Molecular biology methods

THE D173G MUTATION IN ADAMTS-13 CAUSES A SEVERE FORM OF CONGENITAL THROMBOTIC THROMBOCYTOPENIC PURPURA: A CLINICAL, BIOCHEMICAL AND IN SILICO STUDY

Stefano Lancellotti[1#], Flora Peyvandi[2#], Maria Teresa Pagliari[2], Andrea Cairo[2], Safwat Abdel-Azeim[3], Edrisse Chermak[3], Ilaria Lazzareschi[4], Stefano Mastrangelo[4], Luigi Cavallo[3], Romina Oliva[5§] and Raimondo De Cristofaro[1]

[1] Center for Haemorrhagic and Thrombotic Diseases, Department of Medical Sciences, Catholic University School of Medicine, Rome, Italy; [2]Angelo Bianchi Bonomi Hemophilia and Thrombosis Center and Fondazione Luigi Villa, IRCCS Maggiore Hospital, Mangiagalli, Regina Elena Foundation and University of Milan, Milan, Italy; [3] Kaust Catalysis Center, King Abdullah University of Science and Technology, Thuwal 23955-6900, Saudi Arabia; [4] Institute of Pediatrics, Catholic University School of Medicine, Rome, Italy; [5]Department of Sciences and Technologies, University "Parthenope" of Naples, Naples, Italy.

[#] Equal contribution

[§] Senior coauthor

Running title: D173G mutation of ADAMTS-13 and congenital TTP

Word count: 4925

Figure: 8

Tables: 1

Summary word count: 243

Key words: Congenital thrombotic thrombocytopenic purpura; ADAMTS-13; Von Willebrand factor

SUMMARY

Congenital thrombotic thrombocytopenic purpura (TTP) is a rare form of thrombotic microangiopathy, inherited with autosomal recessive mode as a dysfunction or severe deficiency of ADAMTS-13 (A Disintegrin And Metalloprotease with ThromboSpondin 1 repeats Nr. 13), caused by mutations in the ADAMTS-13 gene. About 100 mutations of the ADAMTS-13 gene were identified so far, although only a few characterized by *in vitro* expression studies. A new Asp to Gly homozygous mutation at position 173 of ADAMTS-13 sequence was identified in a family of Romanian origin, with some members affected by clinical signs of TTP. In two male sons, this mutation caused a severe (<3%) deficiency of ADAMTS-13 activity and antigen level, associated with periodic thrombocytopenia, haemolytic anaemia and mild mental confusion. Both parents, who are cousins, showed the same mutation in heterozygous form. Expression studies of the mutant ADAMTS-13, performed in HEK293 cells, showed a severe decrease of the enzyme's activity and secretion, although the protease was detected inside the cells. Molecular dynamics found that in the D173G mutant the interface area between the metalloprotease domain and the disintegrin-like domain significantly decreases during the simulations, while the proline-rich 20 residues linker region (LR, 285-304) between them undergoes extensive conformational changes. Inter-domain contacts are also significantly less conserved in the mutant compared to the wild-type. Both a decrease of the inter-domain contacts along with a substantial conformational rearrangement of LR interfere with the proper maturation and folding of the mutant ADAMTS-13, thus impairing its secretion.

Abbreviations:

ADAMTS-13 (A Disintegrin And Metalloprotease with ThromboSpondin 1 repeats;

CUB: Complement C1r/C1s, Uegf, bone morphogenic protein 1;

CypA and CypB: cyclophilin A and B;

DLD: Disintegrin-like Domain;

HMWm: High Molecular Weight multimers;

IMWm: Intermediate Molecular Weight multimers;

LMWm: Low Molecular Weight multimers;

LR: Proline-Rich 20 residues linker region;

NPT ensemble: the isobaric-isothermal ensemble;

NVT ensemble: ensemble in which number of atoms, volume and temperature are constant;

PPIs: peptidyl-prolyl cis-trans isomerases;

RMSD: root mean square deviation;

RMSF: root mean square fluctuation;

TSP1: ThromboSPondin type 1 repeat;

TTP: Thrombotic Thrombocytopenic Purpura;

UL-VWF Ultra large von Willebrand factor;

VWF: von Willebrand factor.

Amino acids are abbreviated according to the single-letter code

INTRODUCTION

Thrombotic thrombocytopenic purpura (TTP) is an inherited or acquired disorder characterized by the massive formation of platelet thrombi in the microcirculation accompanied by haemolytic anaemia, thrombocytopenia, and clinical and laboratory signs of renal and neurological failure (1, 2). The pathogenesis of TTP is multifactorial: one of the most important factors is the presence in the microcirculation of ultra large multimers of the adhesive glycoprotein von Willebrand factor (UL-VWF), due to the inherited or acquired deficiency of the plasma metalloprotease ADAMTS-13 (A Disintegrin And Metalloprotease with Thrombospondin 1 repeats Nr. 13) that physiologically is the main responsible for the proteolytic processing of VWF multimers and reduction of their size (1). Congenital TTP, also referred to as Upshaw-Schulman syndrome, caused by *ADAMTS-13* mutation and inherited recessively, is a rare form of TTP (3). ADAMTS-13 is a zinc metalloprotease present in plasma at a concentration of about 1 µg/ml (4, 5). The enzyme consists, from the N-terminus, of a relatively short propeptide, the catalytic site, the disintegrin-like (DLD), a first thrombospondin-1 (TSP1) repeat, the Cys-rich domain, the spacer domain, seven TSP1 repeats and 2 CUB (complement components C1r/C1s, urinary Epidermal Growth factor and bone morphogenetic protein-1) domains at the C-terminus (6), whose free thiols have also direct antithrombotic effects (7). When there is a deficiency of this enzyme, uncleaved, ultra large VWF multimers accumulate in microcirculation, causing increased platelet adhesion and aggregation, resulting in the formation of VWF- and platelet-rich thrombi (1, 8, 9). The development of microthrombi results in microangiopathic haemolytic anaemia and causes variable symptoms of organ ischemia and dysfunction (1). Inherited TTP is a rare autosomal recessive disorder due to homozygous or double heterozygous mutations in the ADAMTS-13 gene, causing a severe decrease of ADAMTS-13 level and activity (10-16). About 100 mutations causing inherited ADAMTS-13 deficiency have been identified so far in regions of the gene encoding different domains (10-17) with only a few of them characterized by *in vitro* expression studies (12, 15, 18-22). In this manuscript, we report cases of congenital TTP, due to the homozygous mutation in ADAMTS-13 gene in two young brothers born from two consanguineous parents of Romanian origin. We carried out a molecular investigation on a natural ADAMTS-13 mutant characterized by an Asp to Gly homozygous mutation at position 173 of the metalloprotease, directly engaged in the formation of a low-affinity calcium binding site (23). We explored

the mechanistic effects of this mutation by means of *in vitro* expression studies in mammalian cells with a complete biochemical characterization of this mutant enzyme together with a molecular dynamics (MD) study. We think that the obtained results may help to unravel the role of the mutated site on the ADAMTS-13 calcium binding, conformation and secretion.

Materials and Methods

Case report

The *propositus*, a thirteen year old boy, was admitted to the Department of Pediatric Oncology of the "A. Gemelli" hospital of the Catholic University School of Medicine in Rome, on April 2013 for thrombocytopenia, acute haemolytic crisis, fever and mild mental confusion. The boy, born in Romania, had suffered from haemolysis two years before with similar symptoms. Consanguineity was present in the family history, being the parents cousins and a little brother was dead at age of seven yr. for acute haemolytic crisis, thrombocytopenia and cerebral ischemia. An older brother (21 yr old) periodically suffers from similar episodes of anaemia and thrombocytopenia. The *propositus* was treated with oral steroids with partial resolution of symptoms. During the last acute haemolytic crisis the patient had a severe thrombocytopenia (platelets 11000/μL), fever, jaundice, haematuria and proteinuria.

Direct and indirect Coombs' tests were negative; schistocytes (1-3%) were present in blood smears. Echocardiogram and abdominal scan resulted normal. Coagulation tests (prothrombin time and activated partial thromboplastin time) were normal, whereas von Willebrand factor antigen (VWF:Ag) and activity (VWF:act) showed increased levels (both >140%). In the following days, thrombocytopenia and haematuria were still persistent, with normalization of the renal function indexes (creatinine clearance and renal scintigraphy). Therefore, based on the laboratory data and the clinical course, we monitored the activity and antigen of ADAMTS-13 that resulted <3% using FRET (Fluorescence Resonance Energy Transfer) and ELISA assays, respectively. Moreover,

ELISA testing repeatedly ruled out the presence of anti-ADAMTS-13 antibodies. The activity and antigen levels of ADAMTS-13 were measured in the parents and the brother of the patient, resulting severely deficient in his brother (<3%), whereas ADAMTS-13 antigen and activity levels were 59.5% and 60.9%, respectively, in his father, and 67.5% and 72%, respectively, in his mother (see Table 1). Thus, based on these data and parents consanguineity, a congenital thrombotic thrombocytopenic purpura (Upshaw-Schulman syndrome) was diagnosed. Following a fresh frozen plasma infusion (total dose 800 mL), the monitoring of ADAMTS-13 activity showed a level of 24%. The symptoms of the boy improved progressively, the haematuria and the schistocytes progressively disappeared and at present the patient is periodically receiving fresh frozen plasma infusions, when blood cells controls showed a significant decrease of platelet count (usually every 2/3 weeks). This study was conducted with the patient's consent and approval by the Institutional Review Board of the Catholic University School of Medicine and IRCCS Maggiore Hospital, Mangiagalli and Regina Elena Foundation.

Measurement of ADAMTS-13 activity, ADAMTS-13 antigen, anti-ADAMTS-13antibodies, and VWF levels and multimeric pattern

.

ADAMTS-13 activity was measured in plasma with a FRET assay using the FRETS-VWF86 substrate (Instrumentation Laboratory, Milano, Italy), according to a procedure previously detailed (24). ADAMTS-13 antigen and antibodies neutralizing ADAMTS-13 were measured by commercially available immunoassays (IMUBIND® ADAMTS-13 ELISAand IMUBIND® ADAMTS13 Autoantibody ELISA, American Diagnostica, Milano, Italy).The VWF multimeric pattern was analyzed by SDS-agarose gel electrophoresis (0.8%-1.5% LGT-agarose) as previously reported (24). Von Willebrand factor antigen and activity was measured by immunoassays, using commercially available assays and an automatic chemiluminometer (HemosIL AcuStar von Willebrand Factor Ristocetin Cofactor Activity and HemosIL AcuStar von Willebrand Factor Antigen, both from IL).

Mutation of ADAMTS-13 gene

All DNA analyses were performed with the permission of Ethics Committees of both the sample-collecting hospitals and the institute that performed the gene analysis. Written informed consent was obtained from all patients. DNA was extracted from peripheral blood leukocytes and all the exons and intron–exon boundaries of the ADAMTS-13 gene (NT–017539) were amplified by PCR and sequenced using the ABI Prism Big Dye Terminator Cycle Sequencing Ready Reaction Kit on an ABI Prism 310 Genetic Analyzer (Applied Biosystems, Monza, Italy), as previously detailed (8). The primer sequences and amplification parameters are available on request. The disease-causing *ADAMTS-13* mutations reported here were excluded as common polymorphisms by screening 96 individuals in the general population.

*Plasmid construction***.**

The complete ADAMTS-13 wild-type cDNA was inserted into the mammalian expression vector pcDNA™3.1/V5-His TOPO®TA (Invitrogen, Carlsbad, CA, USA). The p.D173G mutation was introduced into the ADAMTS-13 WT expression vector by site directed mutagenesis using PFU Turbo DNA polymerase (Stratagene, La Jolla, CA, USA) and specifically designed primers. The presence of the mutation was confirmed by sequencing analysis.

Expression studies. For expression studies, ADAMTS-13 WT and mutant p.D173G expression vectors were transiently transfected into human embryonic kidney (HEK) 293 cells, as previously detailed (25). The amount and the activity of WT and mutant recombinant ADAMTS-13 proteins were analysed in the conditioned medium of 6 separate transfections by ELISA and FRET assays, respectively. ADAMTS-13. The amount and the activity of the mutant recombinant ADAMTS-13 are reported as a percentage of WT taken as 100% (± SEM).

ADAMTS-13 model building and analysis

A model has been obtained for the ADAMTS-13 region 81-371, including the catalytic domain and the following ≈100 residues, corresponding to a 20-aa linker and the following DLD. Coordinates of residues 302-322 and 332-371 could be taken from the X-ray structure of a large non-catalytic fragment of

ADAMTS-13 (PDB ID: 3ghm, resolution 2.60 Å (26)). Residues His81 to Pro301 and loop Thr343-Met33, whose coordinates are not present in the 3ghm structure, were comparatively modelled with Modeller v9.12 (27), using a multi-template approach. Structures of ADAMTS1 (PDB ID: 2jih, resolution 2.10 Å (28)), ADAMTS4 (PDB ID: 2rjp, resolution 2.80 Å (29)) and ADAMTS5 (PDB ID: 3hyg, resolution 1.40 Å (30)) have been used as templates, which exhibit a sequence identity with the modelled region of ADAMTS-13 in the range 29-32%. The above structures have been chosen based on resolution and completeness criteria. Using the align module in Modeller, a structural alignment between the three templates was obtained and the ADAMTS-13 sequence was aligned to it. The obtained multiple alignment was then manually adjusted to have Cys242 giving a disulphide bridge with Cys265, analogously to the templates. Coordinates of the three bound calcium ions and one zinc ion have been transferred to the model from the high resolution 3hyg template. The model quality was tested by ProQ (31), finding a LG-score of 4.835 and a MaxSub score of 0.507 (both values above the threshold for very good models), and by Qmean (32), finding a score of 0.631 (Z-score from the distribution of non-redundant high quality structures being only -1.53). The D173G mutant has been obtained by the Pymol mutate tool (33), starting from the model of wild-type ADAMTS-13.

Molecular dynamics simulations

The molecular dynamics (MD) simulations were performed using the GROMACS software (version 4.5.3) (34) with the Amber99SB-ILDN force field (35). Wild-type and D173G ADAMTS-13 mutants were slightly relaxed using 50 steps of steepest descent minimizer. The systems were then immersed in an explicit water box of TIP3P model (36), which extended at least 10 Å away in each direction from any atom of the complex 15933 water molecules were added to both WT and D173G systems. Six and five sodium ions were added to the WT and mutant system, respectively, to neutralize the negative charges, as needed for the particle mesh Ewald calculation (37) of the long-range electrostatic interactions, while a cut-off of 10 Å was used for van der Waals and short-range electrostatic interactions. 500 steps of steepest descent minimization were performed to remove bad contacts with the solvent. All bonds involving hydrogen atoms were constrained by the LINCS algorithm (34). Equilibration of the solvent and ions around the complexes with position constraints of the heavy atoms was performed for 2 ns in the NVT ensemble, followed by 2 ns in the NPT ensemble. NVT simulations were carried out using the velocity rescaling thermostat (V-rescale) (38) and the

NPT ones using Parrinello-Rahman barostat (39). For better sampling, four different 60-ns long NPT MD simulations were performed for each system, assigning different initial velocities. Root mean square deviation (RMSD) and fluctuation (RMSF) values were calculated with standard GROMACS tools. Analysis of the interface area and conservation of the inter-domain contacts along the simulations were performed by the MDcons tool (40). Two thousand snapshots were generated from each trajectory of 60 ns, by writing the coordinates every 30 ps, for the MDcons analyses. An inter-domain contact map was plotted by the COCOMAPS server (40) with the default 8 Å cut-off distance, for two D173G snapshots from the third trajectory, at 0 and 40.46 ns and related information on the interface area and inter-domain H-bonds was also obtained by COCOMAPS.

RESULTS

ADAMTS-13 levels in affected subjects

In the affected subjects ADAMTS-13 activity and antigenic levels were always less than 3%, as measured by FRETS-VWF73. and ELISA testing, respectively (see Table 1). In the acute phase of the disease, the values of VWF antigen and activity were always>140% and accompanied by the presence of ultra large (UL) multimers, as emerged in SDS-agarose gels (see Fig. 1). Notably, in the other affected son, the level of circulating VWF and the multimeric pattern was normal during the periods of clinical remission (see Fig. 1). The parents of the propositus were characterized by intermediate levels of both activity and antigenic levels of ADAMTS-13 (see Table 1), while the multimeric pattern of VWF was normal (Fig. 1).

Genetic analysis

Genetic analysis (nucleotides numbered from the A of the initiation Met codon) identified a new homozygous missense mutation causing substitution at nt 518 (c.519A>G, G**A**C→G**G**C).This mutation caused the substitution of Asp173 to a glycine residue (p.D173G) in the metalloprotease domain of the

ADAMTS-13. The same homozygous mutation was found in the other brother. The two parents were characterized by the same mutation although in heterozygous form.

Expression and activity of the p.D173G mutant in cell cultures

In comparison with the WT rADAMTS-13, the amount of recombinant p.D173G ADAMTS-13 secreted in the conditioned medium of transient transfections was undetectable or at the low sensitivity limit of the assay (3.3 ±2 % [n=6, mean±SEM], Table 1). The activity of the mutant ADAMTS-13 (measured by FRET technique), was always undetectable (<3%). ADAMTS-13 antigen and activity was not detectable (<3%) in the medium of untransfected cells used as a negative control (Table 1). The presence of recombinant WT or p.D173G ADAMTS-13 in the conditioned media and cell lysates was also verified by immunoblotting.

Figure 2 shows that the metalloprotease was detected in both the medium and lysate of cells transfected with the WT ADAMTS-13 expression vector, whereas the mutant p.D137G was detected only in the cell lysates, strongly suggesting a defect in the secretion pathway of the enzyme. The latter finding was in agreement with the lack of ADAMTS-13 antigen and activity observed in the plasma of the congenital TTP patients. The impossibility to obtain sufficient amounts of mutant enzyme in the cell culture medium of transfected cell impeded us to perform an extensive biochemical analysis of structural and functional properties the D173G ADAMTS-13 mutant. Hence, we decided to carry out extended modeling and molecular dynamics studies on this mutant to predict the relevant consequences of the mutation in the metalloprotease.

Modeling

The multiple alignment of ADAMTS1, 4 and 5 used in the modeling procedure of ADAMTS-13 and the obtained 3D model are shown in Figure 3.

Overall fold and comparison with other ADAMTSs

The metalloproteinase domain of ADAMTS-13 is formed by a twisted five strands β-sheet, flanked by three α-helices (α 2, α 4 and α 3). Two additional α -helices are located between β1-strand and helix α2 (α 1) and after a long loop following helix α 4 (α 5). In this domain ADAMTS-13 has overall six cysteine residues in three disulfide bridges that correspond to disulfide bridges that are also observed in ADAMTS-1, -4 and -5. The second one (between Cys202 and Cys281) links the loop region between strands β4 and β5 with a long

loop at the C-terminus of helix α5, which connects the metalloproteinase domain with the DLD and is also involved in the binding of Ca^{2+} ions. Interestingly, as compared to other ADAMTSs of known structure, ADAMTS-13 lacks one disulphide bridge (Cys362-Cys367 in the ADAMTS1 numbering), fixing the orientation of the loop connecting β3 and β4. This is an important loop, shown to be involved in the binding of a Ca^{2+} ion, close to the catalytic site, in ADAMTS-4 and -5 (29, 30) and also shown by alanine scanning mutagenesis experiments to regulate calcium binding and catalytic activity in ADAMTS-13 (23). The two conserved Cys residues in ADAMTS-1, -4 and -5 are substituted in ADAMTS-13 by a glutamate (Glu184) and an arginine (Arg190). Furthermore, the loop in between the above residues is different in sequence and one residue longer in ADAMTS-13, compared to its homologs (Figure 3). That notwithstanding, the calcium binding site is perfectly reproduced in ADAMTS-13, as a salt bridge between Glu184 and Arg190, assisted by a network of H-bonds involving charged and polar residues in the loop, efficiently substitutes the disulphide bridge in fixing the loop orientation. The active site is perfectly conserved in ADAMTS-13, as compared to ADAMTSs of known structure. As for the DLD, that has actually a Cys-like fold (26, 28), it is characterized by four disulphide bridges, like in ADAMTS-1/-4/-5. In it, two short α-helices flank a pair of double-stranded anti parallel β-sheets.

The calcium-binding sites

It is well accepted now that ADAMTS proteins have two calcium binding sites (23), one being occupied by a single Ca^{2+}, the other containing two Ca^{2+} ions, also named Ca-cluster site (23). Both are characterized as usual by the presence of negatively-charged residues (23). The Ca^{++}-cluster site is contributed by the connector loop at the C-terminus of the metalloproteinase domain, by the loop linking helix α3 and strand β3 and by the N-terminus of strand β1. Three aspartate residues and one glutamate are directed involved in the binding with their charged side-chains; additionally, a cysteine participates in the binding with its carbonyl oxygen. These residues are fully conserved between ADAMTS-13 and the homologs whose structures have been used as templates, and correspond to Glu83, Asp166, Asp173 (the mutated residue here), Asp284 and Cys281.

The single calcium-binding site, close to the active site, is instead contributed in ADAMTS-1/-4/-5 by the side-chains of a glutamate at the C-terminus of strand β5 and of an aspartate in a 15-ress loop connecting β3

and β4. These two residues are conserved in ADAMTS-13 and correspond to E212 and D182. Additionally, the above loop participates to the binding through the carbonyl oxygens of other three residues. One of them is conserved in sequence in ADAMTS-13, L183, whereas the other two, R190, V192 are not (Figure 3a). The central region of this loop in ADAMTS-13 has indeed a quite different sequence composition compared to its homologs, and is also one residue longer. As said above, this part of the loop is closed and oriented in ADAMTS-1/-4/-5 by a disulphide bridge that is missing in ADAMTS-13. However, the ADAMTS-13 structure is able to build around the calcium ion a cage that perfectly reproduces the one observed in its homologs. This is due to the fact that the two cysteine residues giving the disulphide bridge are substituted by a glutamate (E184) and an arginine (R190), giving a salt bridge that closes the loop analogously.

Molecular dynamics simulations

To investigate the influence of the D173G mutation on the overall flexibility of ADAMTS-13, we calculated the RMSF of the protein Cα atoms and of the zinc/calcium ions during the simulations. For the WT system, the Cα-RMSF profile of the four different simulations is very similar (see Fig. 4). It is more variable in case of D173G, especially as concerns trajectory 3 (Fig. 4). However, the fluctuation of the mutated residue 173 and of the other calcium binding residues is low, both in the WT and in the mutant (Fig. 4). Analysis of the coordination environment of the calcium bound by D173 evidenced a significant difference between WT and D173G, in the number of protein atoms coordinating the ion (8 and 5-6 for WT and D173G, respectively), as shown in Fig. 5a. At the same time, the number of coordinated water molecules increases to 4-6 in the mutant (from 1 of the WT), depending on the specific simulation (see Fig. 5b). Therefore, in the D173G mutant this Ca^{2+} ion is more solvated and its interaction with the protein is clearly weakened, although from the simulations we don't see the metal ion to leave the binding site. The overall stability of the proteins throughout the MD simulations was monitored through the RMSD of the C□ atoms from the corresponding starting structure. While the WT system remains stable during the 60 ns MD simulations (see Fig. 6) with the RMSD within 3.5 Å and reaching a plateau after roughly 20 ns, for the D173G system, the observed RMSD values are more variable, showing sudden jumps in three out of the four trajectories. To understand the origin of these sudden jumps, indicative of some sharp rearrangement of the structure, we extracted a snapshot from

one trajectory (trajectory 3), corresponding to a peak of the RMSD from the initial structure (exactly at 40.46 ns) and compared it with the initial equilibrated structure. A comparison is shown in Figure 7. From the 3D representations in Figure 7, it is apparent that, although small conformational changes can be observed within the catalytic site of the two snapshots, the main difference concerns the orientation between the catalytic and DLD. As measured by the COCOMAPS server (40), the interface between the catalytic domain (residues 81-286) and the following ≈100 residues is decreased from 1090 to 741 Å^2. It can be seen that contacts between the longer helix region in the DLD (residues 309-314) and a catalytic domain loop around residues 214-216 and between the N-terminus of the downstream helix (around residue 217, not far away in space from the single calcium ion binding site) and the loop region around residue 350 in the DLD are lost. We therefore decided to perform statistical analyses to characterize the interaction between the two domains along the MD simulations. To this aim we used the recently developed MDcons tool (40). As shown in Figure 8, the mutant system features a higher fluctuation in its inter-domain interface area during the simulations, with an average value about 50 Å^2 smaller than the wild-type (1029 vs. 1075 Å^2). In the second half of the simulations, the mutant consistently shows a significant decrease in the interface area, with the average value dropping to 969 Å^2. Another interesting feature is the different conservation of the inter-residue contacts between the domains in the two systems during the MD simulations, which is reflected by the MDcons C50, C70 and C90 coefficients. C50, C70 and C90 represent, respectively, the number of inter-residue contacts conserved in at least 50, 70 and 90% of the analyzed MD frames (see Table S1 in Supplemental Material). Focusing on C70, it assumes values of 0.73 and 0.58, respectively, for the wild-type and mutant system. This means that while the initial inter-domain contacts that are conserved in at least 70% of the wild-type frames amount to 73%, this percentage decreases to 58% for D173G, again highlighting a modified interaction between the two domains in the mutant system.

Discussion

The biochemical and molecular dynamics investigations performed on the natural D173G mutant of ADAMTS-13, responsible for a severe form of Upshaw-Schülman syndrome, allowed to reach some conclusive points: 1) the mutant enzyme is produced but shows a severe secretion defect; 2) the molecular

dynamics simulations showed sudden jumps in the RMSD values in three out of the four performed simulations. This reflects a sharp rearrangement of the mutant structure, especially concerning the orientation between the catalytic site and DLD, while only small conformational changes were observed within the catalytic domain.

The enzymatic activity of ADAMTS-13 depends on divalent metal ions in the following order of potency: $Zn^{2+} > Ca^{2+} > Sr^{2+} > Ba^{2+}$ ions (4, 41). In particular, Ca^{2+} ions are critical for an efficient proteolysis of VWF by ADAMTS-13 (5, 23). ADAMTS-13, analogously to other ADAMTS proteins, has two calcium binding sites, for a total of three calcium ions bound (5, 23). Asp173 and other residues involved in calcium-binding in the so-named "Ca^{++}-cluster site" are widely conserved within the ADAMTS family. Previous studies found that Ca^{2+} binding to this site causes a spectroscopic response measurable by an absorbance increase at 280 nm under low-ionic-strength conditions (23). This spectroscopic response was attributed to a conformational change in the metalloprotease domain of ADAMTS-13. No absorbance change was instead measured when Ca^{2+} ion was added to Ala-mutants of E83, D173, C281, and D284 (23), suggesting that the lack of Ca^{2+}-dependent conformational change had been caused by the introduction of those mutations. The process of conformational change induced by calcium binding to this site might involve repositioning of the more C-terminal domains (starting from the disintegrin-like one) to align with the active site of the metalloprotease. A regulatory role was indeed proposed for the ADAMTS DLD, given its proximity to the catalytic site (28). Recently, based on mutagenesis studies, a possible exosite (exosite 1) for VWF recognition has been located in the DLD of ADAMTS-13, including residues R349 and P353 (26) . It was also interestingly shown that altering the interaction between the catalytic and the DLD in ADAMTS-13 can cause catalytic and/or secretion defects (23, 26, 42, 43). The present data show that the D173G mutant is not or minimally secreted into the medium or plasma *in vivo*. The cause of the defective secretion is still unclear. ADAMTS-13 undergoes extensive maturation in endoplasmic reticulum (ER) and is heavily glycosylated (44). In particular, the O-fucosylation occurring at 6 TSP1 repeats of ADAMTS13 and the N-glycosylation process appear to be critical for folding, secretion and proteolytic activity of ADAMTS-13 (45). The protein folding machinery of the ER consists of three major classes of proteins: (i) foldases, (ii) molecular chaperones, and (iii) the oligosaccharide processing enzymes as well as lectin chaperones calnexin and calreticulin, which all are involved in protein quality control (46). Among the foldases, the peptidyl-prolyl

cis-trans isomerases (PPIs) are important, particularly in large proteins with significant numbers of proline residues. The isomerization of peptidyl-prolyl bonds is a rate-limiting step during protein folding and would spontaneously occur at a rate too slow to support efficient protein folding in the cell (47). Catalysis of proline cis-trans isomerization is therefore often a necessary step required for accurate protein folding *in vivo*. Mammalian cells contain three classes of PPIs: parvulins, cyclophilins (Cyps), and FK506-binding proteins (48). ADAMTS13, harboring 118 prolines, contains a higher number of proline residues and thus needs PPIases activity to fold and maturate correctly in the cell. Cyclophilins, most notably cyclophilin A and B (CypA and CypB), constitute an important family of PPIases. The linker region between the catalytic site and the DLD (residues 285-304) contains numerous Pro residues (7 out of 20 residues (35%), see Fig.3). Thus, based on the MD results, it is likely that the vast conformational transitions of the linker region associated with the D173G mutation would impair the molecular recognition and the foldase activity of CypA and CypB.

Although this natural mutation clearly causes a severe defect of secretion, this study cannot establish whether or not the activity of the metalloprotease inside the cell is maintained. This issue will be addressed by means of more complex in vitro co-expression studies, as previously reported (49). In conclusion, this study shows that the D173G mutant shows a) a severe defect of its secretion; b) weakening of coordination of the two Ca^{2+} ions in the Ca-cluster site linked to c) a vast rearrangement of the contacts between the catalytic domain and the DLD. The clinical course of this severe defect of ADAMTS-13 is dominated by fluctuating episodes of thrombocytopenia and microcirculation ischemia. The inconstant occurrence of thrombocytopenia and microcirculatory thrombosis, despite the severe genetic defect of ADAMTS-13, could derive from a substantial release of high molecular weight VWF multimers in occasion of certain clinical settings, such as inflammatory and/or infectious diseases. This hypothesis was verified and confirmed anamnestically by the patient's available clinical reports. The biochemical and MD studies herein reported clearly show that the D173G mutation negatively affects the conformational equilibrium of the enzyme and, likely, the biochemical mechanisms involved in the folding, trafficking and secretion of the protease.

Acknowledgments

Stefano Lancellotti, performed analytical measurements;
Ilaria Lazzareschi and Stefano Mastrangelo: enrolled and characterized patients;
Safwat Abdel-Azeim, Edrisse Chermak, Luigi Cavallo and Romina Oliva: performed molecular modeling and molecular dynamics measurements and drafted the paper;
Maria Teresa Pagliari and Andrea Cairo, performed genetic analysis and expression studies;
Flora Peyvandi, analyzed data and revised the paper;
Raimondo De Cristofaro designed the study, analyzed data, performed some VWF measurements and drafted the paper.

All the Authors revised and contributed to the final version of the manuscript.

Sources of Funding

This work has been in part supported by the Catholic University School of Medicine to RDC grant "Linea D1" 2012/2013" and grant "Linea D1" 2013-2014. The study was supported by the Italo Monzino Foundation (FP).

Disclosures: None.

References

1. Moake JL. Thrombotic microangiopathies. N Engl J Med 2002 Aug 22;347(8):589-600.
2. Vesely SK, George JN, Lammle B, et al. ADAMTS13 activity in thrombotic thrombocytopenic purpura-hemolytic uremic syndrome: relation to presenting features and clinical outcomes in a prospective cohort of 142 patients. Blood 2003 Jul 1;102(1):60-8.
3. Levy GG, Nichols WC, Lian EC, et al. Mutations in a member of the ADAMTS gene family cause thrombotic thrombocytopenic purpura. Nature 2001 Oct 4;413(6855):488-94.
4. Zheng X, Chung D, Takayama TK, et al. Structure of von Willebrand factor-cleaving protease (ADAMTS13), a metalloprotease involved in thrombotic thrombocytopenic purpura. J Biol Chem 2001 Nov 2;276(44):41059-63.
5. Tsai HM. Physiologic cleavage of von Willebrand factor by a plasma protease is dependent on its conformation and requires calcium ion. Blood 1996 May 15;87(10):4235-44.
6. Chung DW, Fujikawa K. Processing of von Willebrand factor by ADAMTS-13. Biochemistry 2002 Sep 17;41(37):11065-70.
7. Bao J, Xiao J, Mao Y, et al. Carboxyl terminus of ADAMTS13 directly inhibits platelet aggregation and ultra large von Willebrand factor string formation under flow in a free-thiol-dependent manner. Arterioscler Thromb Vasc Biol 2014 Feb;34(2):397-407.
8. Peyvandi F, Lavoretano S, Palla R, et al. Mechanisms of the interaction between two ADAMTS13 gene mutations leading to severe deficiency of enzymatic activity. Hum Mutat 2006 Apr;27(4):330-6.

9. Peyvandi F, Lavoretano S, Palla R, et al. ADAMTS13 and anti-ADAMTS13 antibodies as markers for recurrence of acquired thrombotic thrombocytopenic purpura during remission. Haematologica 2008 Feb;93(2):232-9.
10. Assink K, Schiphorst R, Allford S, et al. Mutation analysis and clinical implications of von Willebrand factor-cleaving protease deficiency. Kidney Int 2003 Jun;63(6):1995-9.
11. Bestetti G, Stellari A, Lattuada A, et al. ADAMTS 13 genotype and vWF protease activity in an Italian family with TTP. Thromb Haemost 2003 Nov;90(5):955-6.
12. Kokame K, Miyata T. Genetic defects leading to hereditary thrombotic thrombocytopenic purpura. Semin Hematol 2004 Jan;41(1):34-40.
13. Licht C, Stapenhorst L, Simon T, et al. Two novel ADAMTS13 gene mutations in thrombotic thrombocytopenic purpura/hemolytic-uremic syndrome (TTP/HUS). Kidney Int 2004 Sep;66(3):955-8.
14. Studt JD, Kremer Hovinga JA, Antoine G, et al. Fatal congenital thrombotic thrombocytopenic purpura with apparent ADAMTS13 inhibitor: in vitro inhibition of ADAMTS13 activity by hemoglobin. Blood 2005 Jan 15;105(2):542-4.
15. Uchida T, Wada H, Mizutani M, et al. Identification of novel mutations in ADAMTS13 in an adult patient with congenital thrombotic thrombocytopenic purpura. Blood 2004 Oct 1;104(7):2081-3.
16. Veyradier A, Lavergne JM, Ribba AS, et al. Ten candidate ADAMTS13 mutations in six French families with congenital thrombotic thrombocytopenic purpura (Upshaw-Schulman syndrome). J Thromb Haemost 2004 Mar;2(3):424-9.
17. Lancellotti S, Basso M, De Cristofaro R. Proteolytic Processing of Von Willebrand Factor by Adamts13 and Leukocyte Proteases. Mediterr J Hematol Infect Dis 2013;5(1):e2013058.
18. Plaimauer B, Fuhrmann J, Mohr G, et al. Modulation of ADAMTS13 secretion and specific activity by a combination of common amino acid polymorphisms and a missense mutation. Blood 2006 Jan 1;107(1):118-25.
19. Lotta LA, Garagiola I, Palla R, et al. ADAMTS13 mutations and polymorphisms in congenital thrombotic thrombocytopenic purpura. Hum Mutat 2010 Jan;31(1):11-9.
20. Camilleri RS, Scully M, Thomas M, et al. A phenotype-genotype correlation of ADAMTS13 mutations in congenital thrombotic thrombocytopenic purpura patients treated in the United Kingdom. J Thromb Haemost 2012 Sep;10(9):1792-801.
21. Donadelli R, Banterla F, Galbusera M, et al. In-vitro and in-vivo consequences of mutations in the von Willebrand factor cleaving protease ADAMTS13 in thrombotic thrombocytopenic purpura. Thromb Haemost 2006 Oct;96(4):454-64.
22. De Cristofaro R, Peyvandi F, Baronciani L, et al. Molecular mapping of the chloride-binding site in von Willebrand factor (VWF): energetics and conformational effects on the VWF/ADAMTS-13 interaction. J Biol Chem 2006 Oct 13;281(41):30400-11.
23. Gardner MD, Chion CK, de Groot R, et al. A functional calcium-binding site in the metalloprotease domain of ADAMTS13. Blood 2009 Jan 29;113(5):1149-57.
24. Oggianu L, Lancellotti S, Pitocco D, et al. The oxidative modification of von Willebrand factor is associated with thrombotic angiopathies in diabetes mellitus. PLoS One 2013;8(1):e55396.
25. De Cristofaro R, Peyvandi F, Palla R, et al. Role of chloride ions in modulation of the interaction between von Willebrand factor and ADAMTS-13. J Biol Chem 2005 Jun 17;280(24):23295-302.
26. Akiyama M, Takeda S, Kokame K, et al. Crystal structures of the noncatalytic domains of ADAMTS13 reveal multiple discontinuous exosites for von Willebrand factor. Proc Natl Acad Sci U S A 2009 Nov 17;106(46):19274-9.
27. Sali A, Blundell TL. Comparative protein modelling by satisfaction of spatial restraints. Journal of molecular biology 1993 Dec 5;234(3):779-815.
28. Gerhardt S, Hassall G, Hawtin P, et al. Crystal structures of human ADAMTS-1 reveal a conserved catalytic domain and a disintegrin-like domain with a fold homologous to cysteine-rich domains. J Mol Biol 2007 Nov 2;373(4):891-902.
29. Mosyak L, Georgiadis K, Shane T, et al. Crystal structures of the two major aggrecan degrading enzymes, ADAMTS4 and ADAMTS5. Protein Sci 2008 Jan;17(1):16-21.
30. Shieh HS, Mathis KJ, Williams JM, et al. High resolution crystal structure of the catalytic domain of ADAMTS-5 (aggrecanase-2). The Journal of biological chemistry 2008 Jan 18;283(3):1501-7.
31. Wallner B, Elofsson A. Can correct protein models be identified? Protein science : a publication of the Protein Society 2003 May;12(5):1073-86.

32. Benkert P, Kunzli M, Schwede T. QMEAN server for protein model quality estimation. Nucleic acids research 2009 Jul;37(Web Server issue):W510-4.
33. DeLano Scientific L. http://wwwpymolorg 2002.
34. Hess B, Bekker H, Berendsen HJC, et al. LINCS: A linear constraint solver for molecular simulations. Journal of Computational Chemistry 1997 Dec 1;18(12):1463.
35. Lindorff-Larsen K, Piana S, Palmo K, et al. Improved side-chain torsion potentials for the Amber ff99SB protein force field. Proteins 2010 Jun;78(8):1950-8.
36. Jorgensen WL, Duffy EM, Tiradorives J. Comparison of simple potential functions for simulating liquid water J Chem Phys 1983 Jul 15;83(2):926.
37. Darden T, York D, Pedersen L. Particle Mesh Ewald - an N.Log(N) Method for Ewald Sums in Large Systems. J Chem Phys 1993 Jun 15;98(12):10089.
38. Bussi G, Donadio D, Parrinello M. Canonical sampling through velocity rescaling. J Chem Phys 2007 Jan 7;126(1):014101.
39. Parrinello M, Rahman A. Polymorphic Transitions in Single-Crystals - a New Molecular-Dynamics Method. J Appl Phys 1981 Dec 1;52(12):7182.
40. Abdel-Azeim S, Chermak E, Vangone A, et al. MDcons: Intermolecular contact maps as a tool to analyze the interface of protein complexes from molecular dynamics trajectories. BMC Bioinformatics 2014;15 Suppl 5:S1.
41. Furlan M, Robles R, Lammle B. Partial purification and characterization of a protease from human plasma cleaving von Willebrand factor to fragments produced by in vivo proteolysis. Blood 1996 May 15;87(10):4223-34.
42. Crawley JT, de Groot R, Xiang Y, et al. Unraveling the scissile bond: how ADAMTS13 recognizes and cleaves von Willebrand factor. Blood 2011 Sep 22;118(12):3212-21.
43. de Groot R, Bardhan A, Ramroop N, et al. Essential role of the disintegrin-like domain in ADAMTS13 function. Blood 2009 May 28;113(22):5609-16.
44. Liu T, Qian WJ, Gritsenko MA, et al. Human plasma N-glycoproteome analysis by immunoaffinity subtraction, hydrazide chemistry, and mass spectrometry. J Proteome Res 2005 Nov-Dec;4(6):2070-80.
45. Zhou W, Tsai HM. N-Glycans of ADAMTS13 modulate its secretion and von Willebrand factor cleaving activity. Blood 2009 Jan 22;113(4):929-35.
46. Ricketts LM, Dlugosz M, Luther KB, et al. O-fucosylation is required for ADAMTS13 secretion. J Biol Chem 2007 Jun 8;282(23):17014-23.
47. Hebert DN, Molinari M. In and out of the ER: protein folding, quality control, degradation, and related human diseases. Physiol Rev 2007 Oct;87(4):1377-408.
48. Stevens FJ, Argon Y. Protein folding in the ER. Semin Cell Dev Biol 1999 Oct;10(5):443-54.
49. Majerus EM, Zheng X, Tuley EA, et al. Cleavage of the ADAMTS13 propeptide is not required for protease activity. J Biol Chem 2003 Nov 21;278(47):46643-8.

Figure legends

Figure 1.
Discontinuous (0.8-1.5%) SDS-agarose gels of VWF samples from the members of ~~the family~~ of the propositus' family.
PNP is normal pooled plasma from ten different healthy subjects. All the samples, whose VWF:Ag level in plasma is reported at the bottom of the Figure, were similarly diluted 1:20 in the sample buffer and 20 µl were loaded on each lane. -Lane 1 and 2 show samples taken in two different occasions during the hospitalization of the propositus. ~~The same amount of VWF antigen was used in each lane (1 µg)~~. Although the final amount of VWF multimers loaded on each line was comparable, (even if it was slightly higher in lane 2), ~~not exactly the same,~~ ~~the presence of high~~ ultra-large molecular weight VWF multimers (~~HMW-~~UL-VWF) ~~UL multimers~~ are visible only in the lane pertaining to the son with homozygous mutation during acute phase of the disease (plts = 20000/µL). Instead, the plasma sample of his brother was taken during a remission period when the platelet count was normal (178000/µL).

Figure 2. Western blotting of ADAMTS-13 in both medium and lysate of HEK-293 cells transfected with both WT and mutant D173G gene. Not transfected cells (c-) were used as negative control.

Figure 3. Multiple alignment and 3D model. a) The multiple alignment between ADAMTS-13 and ADAMTS-1/-4/-5 used in the comparative modelling procedure. The reported numbering corresponds to ADAMTS-13. Experimental coordinates were available for ADAMTS-13 residues shadowed in grey (PDB ID: 3ghm). Residues in the catalytic site are shadowed in magenta. Residues involved in calcium binding in the Ca-cluster site are shadowed dark and light blue, if involved in binding with their side-chain or main-chain, respectively. Analogously, residues involved in binding the single calcium ion are shadowed dark and light green, if binding with their side-chain or main-chain, respectively. The Cys residue involved in a conserved disulphide bridge in the templates and substituted by a Glu in ADAMTS-13 is colored yellow. Pro residues in the linker between the catalytic and the disintegrin-like domains are highlighted in red. Asp173, undergoing mutation to Ala or Gly is outlined by a star. **b)** ADAMTS-13 3D model, top view of the catalytic domain. Zinc and calcium ions are colored blue and orange, respectively. Residues colored in the alignment are similarly colored in the 3D model and shown in a stick representation. The mutated Asp173 is labeled.

Figure 4. The calculated RMSF of Cα atoms vs. protein residue number during the simulations for: WT (top) and D173G (bottom) ADAMTS13. The four simulations are shown in different colors. The mutated residue is indicated by an arrow. Residues binding a calcium ion with their side-chains are outlined by a star. The active site (as) is also labelled. Fluctuation of residues in the active site is particularly low, with an appreciable increase only in the D173G third trajectory. The position of all the ions is well fixed, with maximum RMSF values below 0.5 Å.

Figure 5. A) Analysis of the coordination environment around the Ca^{2+} coordinated by residue 173.
Left, radial distribution function (solid line) of water molecules around Ca^{2+}, and the corresponding Ca^{2+} coordination number (dashed line). Right, Ca^{2+} coordination number by protein atoms. Analysis of the

coordination environment of the Ca^{2+} bound by D173 in the WT indicates that in the four simulations of the WT this Ca^{2+} is firmly coordinated by 8 atoms from the protein, with only one water molecule able to coordinate to it. **B) Analysis of the coordination environment around the Ca^{2+} coordinated by residue 173 in the D173G mutant.** Left, radial distribution function (solid line) of water molecules around Ca^{2+} 293, and the corresponding Ca^{2+} 293 coordination number (dashed line). Right, Ca^{2+} 293 coordination number by protein atoms.

Figure 6. Time dependence of RMSDs for the Cα of WT (top) and D173G ADAMTS-13 (bottom) in the 60-ns MD simulations. The four simulations are shown in different colors.

Figure 7. Comparison between the initial ADAMTS-13 D173G system (0 ns) and a snapshot at 40.46 ns (trajectory 3). Top : inter-domain contact maps as obtained by COCOMAPS. Bottom : 3D representation, with catalytic domain in blue, but for the mutated residue that is red, and remaining residues in hotpink. Zinc and calcium ions are shown as cyan and orange spheres, respectively. The single H-bond between the catalytic site and DLD, involving the side chain of Arg180, immediately upstream of the loop binding the single calcium ion, and the backbone of Val313 in the longer DLD helix, is also lost, while the network of H-bonds between the catalytic domain and the inter-domain linker is substantially changed.

Figure 8. Interface area of the two WT and mutant systems along the MD simulations. For each system, values have been averaged over the four calculated trajectories.

Table 1. ADAMTS-13 and Von Willebrand factor level in plasma of the propositus, his brother and their parents

Subject	Age (yr)	ADAMTS-13 activity (FRET assay, %)	ADAMTS-13 antigen (ELISA, %)	VWF:Ag (%)	VWF:act (%)
Propositus	13	<3*	<1	140.2	143.1
Brother	22	<3*	<1	84.8	90.1
Father	51	60.9	59.5	89.8	107
Mother	50	72	67.5	140	164.3

ADAMTS-13 antigen and activity level in the conditioned media ~~and lysates~~ of HEK293 cells transfected with WT and mutant expression vectors.

rADAMTS13	Antigen Levels (%±SEM§)	Activity Levels (%±SEM)
WT	100	100
p.D173G	3.3±2	<3*
Untransfected cells	2±2	<3*

Results are expressed as the percentage of WT ADAMTS-13 (n=6, mean±SEM).

* Lower limit of sensitivity of FRET assay.

§ SEM: Standard Error of the Mean

Formatted: Superscript

Formatted: Superscript

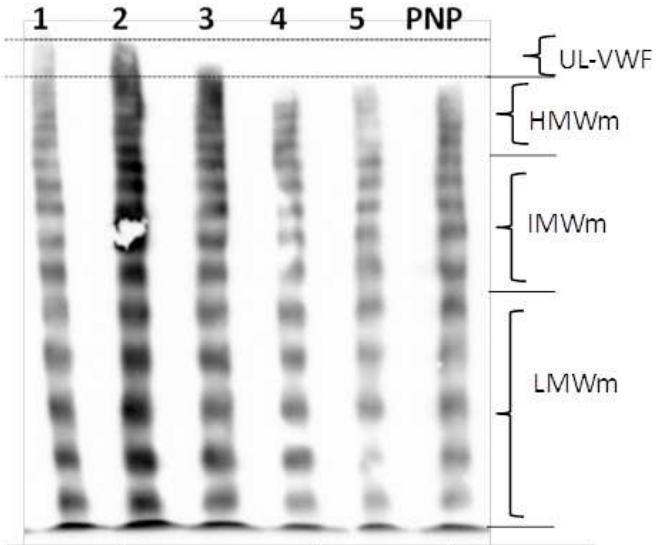

Lane	Identity	VWF:Ag (%)	VWF:act (%)
1	Propositus-hospital	140	143.1
2	Propositus-hospital	182	199
3	Mother	140	164.3
4	Father	89.8	107.9
5	Brother	84.8	90.1
6	PNP	100	99

Figure 1

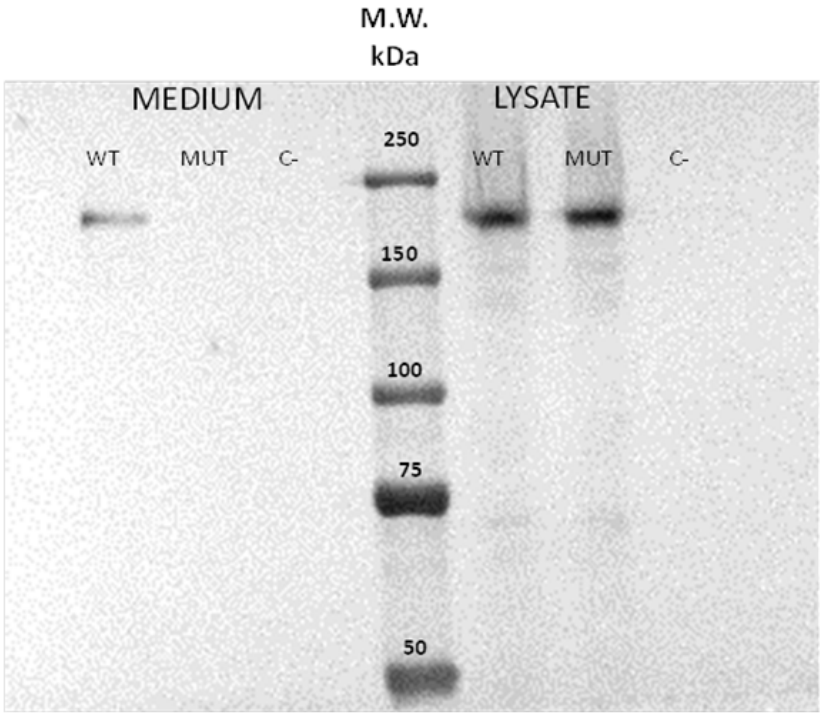

Figure 2

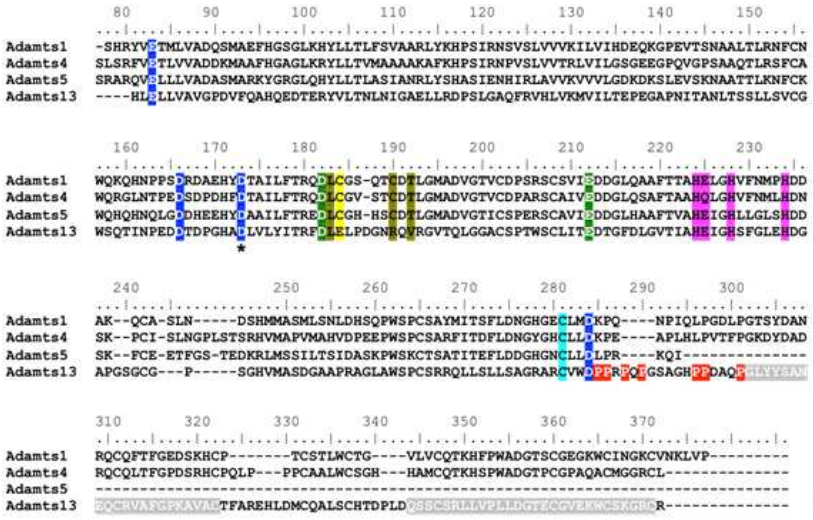
Adamts1
Adamts4
Adamts5
Adamts13

a)

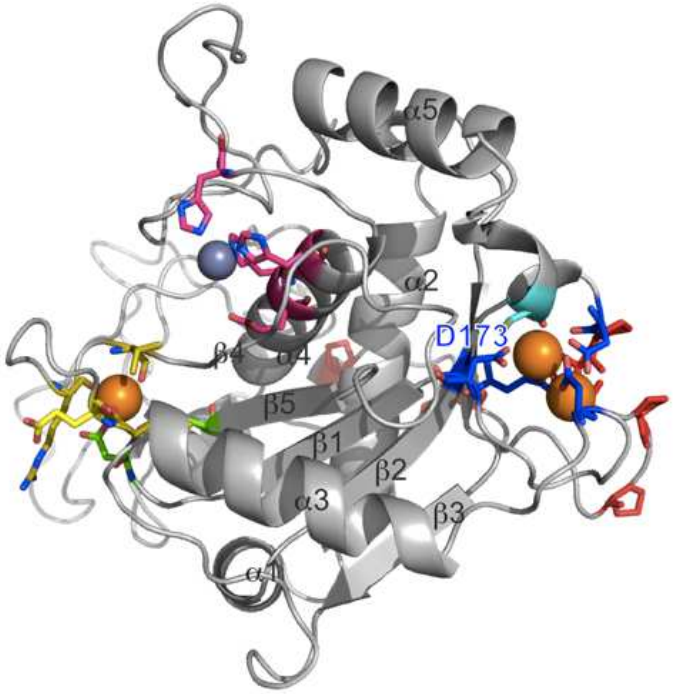
α5
α2
D173
β4
α4
β5
β1
β2
α3
β3
α1

b)

Figure 3

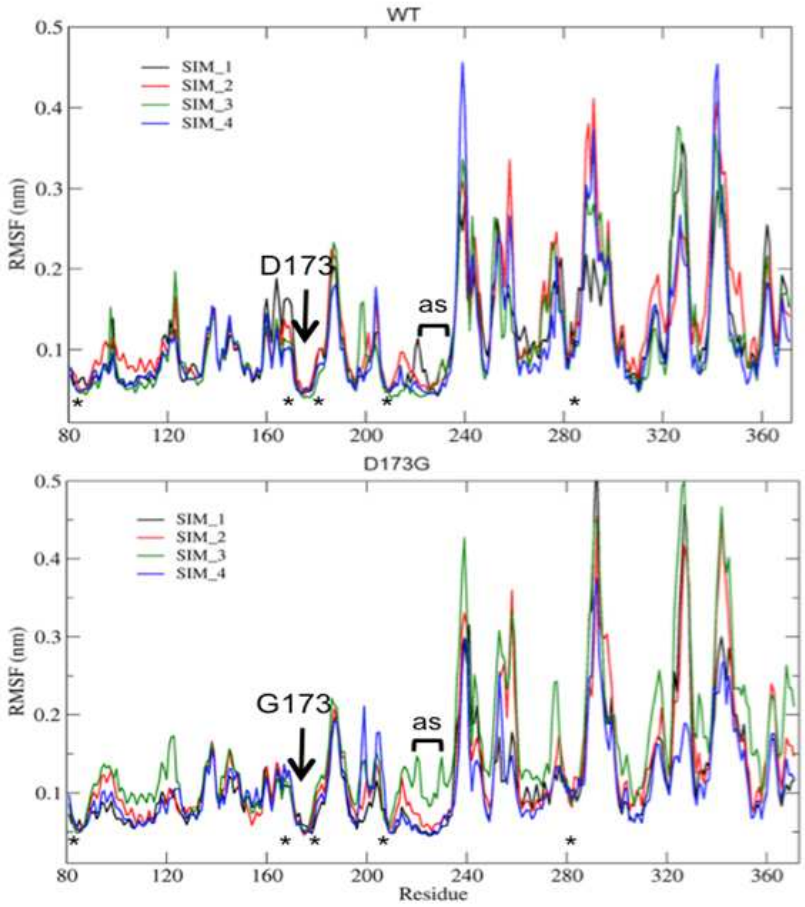

Figure 4

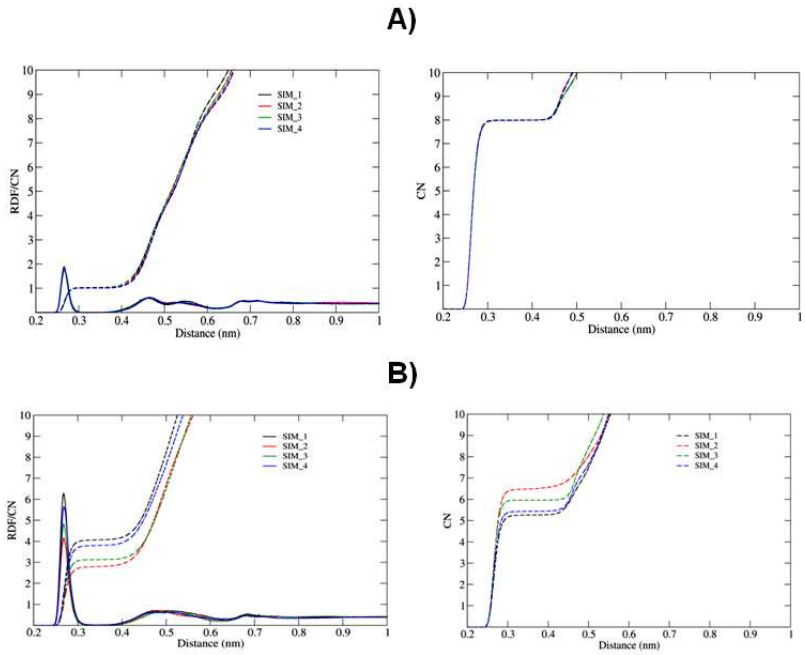

Figure 5

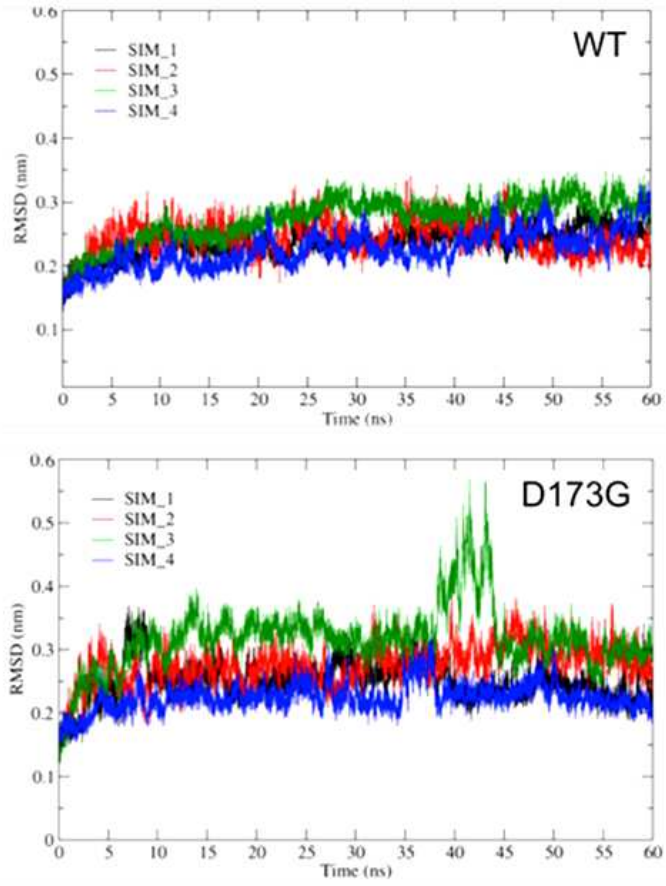
WT
SIM_1
SIM_2
SIM_3
SIM_4
RMSD (nm)
Time (ns)
D173G
SIM_1
SIM_2
SIM_3
SIM_4
RMSD (nm)
Time (ns)

Figure 6

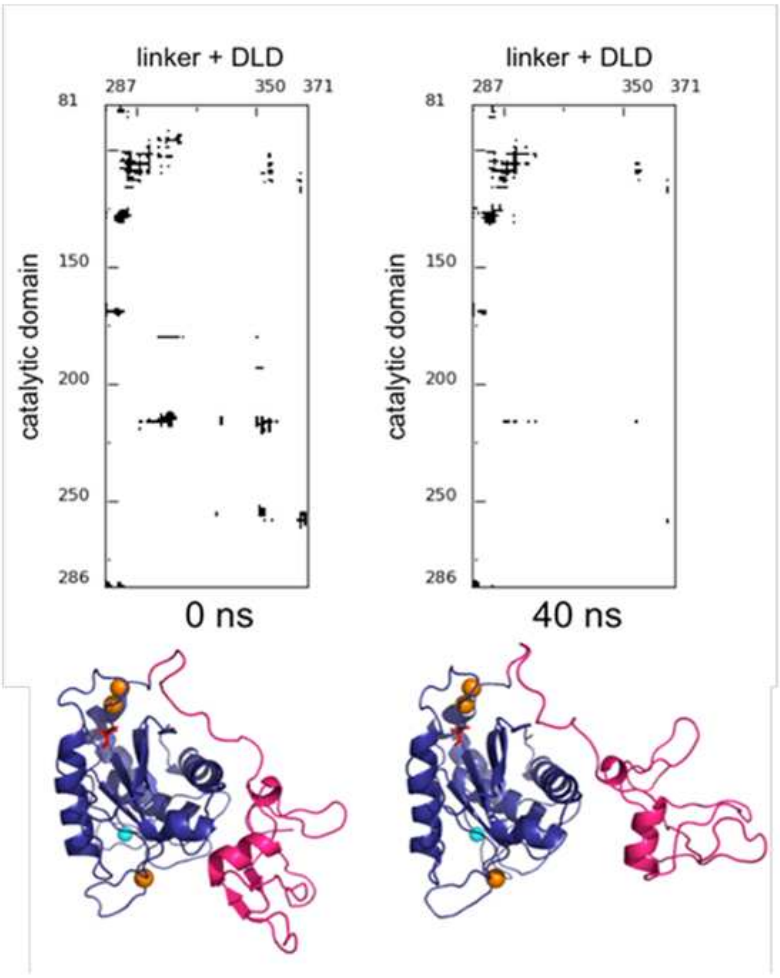
linker + DLD
287
350
371
81
150
200
250
286
catalytic domain
0 ns
linker + DLD
287
350
371
81
150
200
250
286
catalytic domain
40 ns

Figure 7

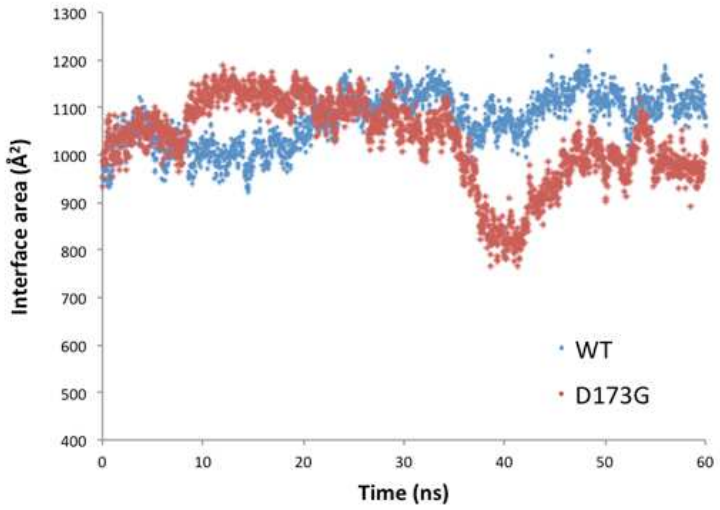
Interface area (Å²)
1300
1200
1100
1000
900
800
700
600
500
400
0
10
20
30
40
50
60
Time (ns)
WT
D173G

Figure 8

Extra Table

What is known about this topic?

• Congenital thrombotic thrombocytopenic purpura is caused by mutations of ADAMTS-13 gene
• About 100 natural mutations of ADAMTS-13 gene were found, although only a few were characterized from a biochemical standpoint

What does this paper add?

• The present study demonstrates for the first time that the natural D173G mutation in the catalytic domain of ADAMTS13, never described before, causes a severe form of Upshaw-Schülman syndrome
• Biochemical and molecular dynamics studies showed that the D173G mutation severely alters the inter-domain contacts between the catalytic and the disintegrin-like domains, and negatively affects the mechanisms of intracellular folding trafficking and secretion of the enzyme.